

Review

Open Access



Challenges and strategies in catalysts design towards efficient and durable alkaline seawater electrolysis for green hydrogen production

Jaehyun Kim¹, Jin Ho Seo¹, Jae Kwan Lee¹, Myoung Hwan Oh^{2,*}, Ho Won Jang^{1,3,*} 

¹Department of Materials Science and Engineering, Research Institute of Advanced Materials, Seoul National University, Seoul 08826, Republic of Korea.

²Department of Energy Engineering, KENTECH Institute for Environmental and Climate Technology, Korea Institute of Energy Technology, Naju 58330, Republic of Korea.

³Advanced Institute of Convergence Technology, Seoul National University, Suwon 16229, Republic of Korea.

***Correspondence to:** Prof. Myoung Hwan Oh, Department of Energy Engineering, KENTECH Institute for Environmental and Climate Technology, Korea Institute of Energy Technology, 21 KENTECH-gil, Naju 58330, Republic of Korea. E-mail: mhoh@kentech.ac.kr; Prof. Ho Won Jang, Department of Materials Science and Engineering, Research Institute of Advanced Materials, Seoul National University, 1 Gwanak-ro, Gwanak-gu, Seoul 08826, Republic of Korea; Advanced Institute of Convergence Technology, Seoul National University, 145 Gwanggyo-ro, Yeongtong-gu, Suwon 16229, Republic of Korea. E-mail: hwjang@snu.ac.kr

How to cite this article: Kim, J.; Seo, J. H.; Lee, J. K.; Oh, M. H.; Jang, H. W. Challenges and strategies in catalysts design towards efficient and durable alkaline seawater electrolysis for green hydrogen production. *Energy Mater.* **2025**, 5, 500076. <https://dx.doi.org/10.20517/energymater.2024.220>

Received: 21 Oct 2024 **First Decision:** 18 Dec 2024 **Revised:** 4 Jan 2025 **Accepted:** 15 Jan 2025 **Published:** 21 Mar 2025

Academic Editor: Sining Yun **Copy Editor:** Fangling Lan **Production Editor:** Fangling Lan

Abstract

Seawater electrolysis offers a sustainable solution for hydrogen production by utilizing ocean water as an electrolyte. However, the chlorine evolution reaction (CIER) and the accumulation of magnesium and calcium precipitates pose significant challenges to efficiency and durability. CIER competes with the oxygen evolution reaction, reducing hydrogen output and accelerating electrode degradation, while precipitate formation on the cathode blocks catalytic sites and impairs long-term performance. Anion exchange membrane water electrolyzers tackle these challenges by leveraging alkaline media to suppress CIER and enhance catalyst stability. Recent advances in selective catalysts, protective coatings, and alternative oxidation reactions further improve reaction selectivity and energy efficiency. Additionally, strategies such as surface engineering and pH modulation mitigate precipitate formation, ensuring stable operation. Scaling these innovations into anion exchange membrane water electrolyzer systems demonstrates their potential for industrial-level hydrogen production. By overcoming



© The Author(s) 2025. **Open Access** This article is licensed under a Creative Commons Attribution 4.0 International License (<https://creativecommons.org/licenses/by/4.0/>), which permits unrestricted use, sharing, adaptation, distribution and reproduction in any medium or format, for any purpose, even commercially, as long as you give appropriate credit to the original author(s) and the source, provide a link to the Creative Commons license, and indicate if changes were made.



fundamental challenges and practical barriers, seawater electrolysis advances toward commercial deployment and a sustainable energy future.

Keywords: Green hydrogen, seawater electrolysis, oxygen evolution reaction, non-noble metal catalysts, electrocatalysis, water splitting

INTRODUCTION

Green hydrogen is a clean and scalable energy carrier produced through water electrolysis powered by renewable energy. It offers a sustainable solution for decarbonizing industries, transportation, and power generation. While alkaline water electrolysis (AWE) remains the most established method due to its technical maturity and cost-effectiveness, it depends on high-purity water, limiting its practicality in regions where freshwater is scarce. Seawater, which accounts for over 96% of global water resources, exhibits a superior conductivity (5 S m^{-1}) compared to pure water ($5.5 \times 10^{-6} \text{ S m}^{-1}$) and maintains a slightly alkaline pH range of 7.5–8.5, positioning it as a promising natural electrolyte^[1]. Therefore, direct seawater electrolysis provides a promising alternative by utilizing an abundant and accessible feedstock^[2–6]. This approach is especially attractive for large-scale hydrogen production in coastal areas and regions facing freshwater limitations.

Despite its potential, seawater electrolysis faces major challenges, including the competitive chlorine evolution reaction (ClER) and the accumulation of magnesium hydroxide ($\text{Mg}(\text{OH})_2$) and calcium carbonate (CaCO_3) precipitates^[7–9]. These issues undermine system efficiency, increase maintenance requirements, and shorten the lifespan of electrolyzers. Figure 1 highlights these challenges by illustrating ClER at the anode and the formation of Mg^{2+} and Ca^{2+} deposits at the cathode. The simultaneous occurrence of these two issues creates significant barriers to the long-term stability and commercial viability of seawater electrolyzers.

Chlorine evolution competes with the desired oxygen evolution reaction (OER) at the anode, particularly under the high voltages required to sustain industrial current densities. This side reaction not only reduces hydrogen production efficiency but also accelerates the corrosion of catalytic surfaces, threatening system durability. At the cathode, the rise in local pH during the hydrogen evolution reaction (HER) leads to the precipitation of $\text{Mg}(\text{OH})_2$ and CaCO_3 , which block active sites and hinder electrochemical performance^[10–13], considering the chemical composition of natural seawater shown in Table 1^[14,15]. Managing these challenges requires balancing OER selectivity and ClER suppression while preventing fouling at the cathode. The performance of the reported electrocatalysts for AEMWE utilizing seawater as the electrolyte is summarized in Table 2^[16–25].

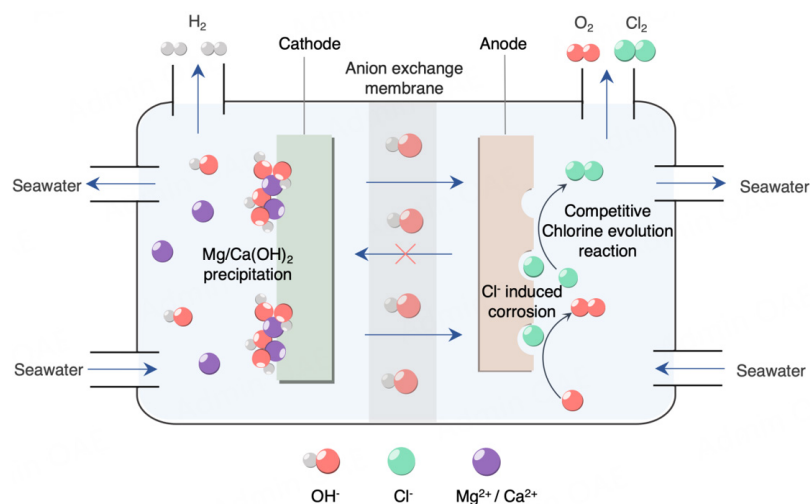
Researchers have developed several strategies to mitigate these issues. Catalyst designs that promote OER over ClER through both thermodynamic and kinetic approaches have shown significant promise^[26–30]. For example, the use of protective coatings, such as manganese oxide, can repel chloride ions while stabilizing catalytic surfaces^[31]. Additionally, advanced electrode designs focus on modifying local chemical environments to prevent ClER while ensuring efficient hydrogen evolution. Similar progress has been made in tackling precipitation challenges through hydrophobic coatings, membrane technologies, and ion-exchange systems, which limit the formation of insoluble deposits during electrolysis. To address these challenges holistically, innovative system designs have integrated alternative oxidation reactions, such as hydrazine oxidation, into seawater electrolysis. These systems operate at lower voltages, reducing the risk of ClER while enhancing energy efficiency.

Table 1. Chemical composition of impurities in natural seawater^[14,15]

Element	Cl ⁻	Na ⁺	Mg ²⁺	SO ₄ ²⁻	Ca ²⁺	K ⁺	Br ⁻
Concentration (ppm)	19,500-22,000	107,70-14,039	1,290-1,490	905-3,200	378-421	380-469	67

Table 2. Comparison of the state-of-the-art electrocatalysts for AEMWE using seawater as an electrolyte

Catalysts	Electrolyte	Current density@1.8 V _{RHE}	Stability	Ref.
RuMoNi RuMoNi	6 M KOH + seawater, 80 °C	1,500 mA cm ⁻²	240 h	[16]
Pt/C NiFeCo-LDH	1 M KOH + seawater, 50 °C	1,500 mA cm ⁻²	50 h	[17]
Ru/P-MoB/NiFe RuO ₂ /NiFe	1 M KOH + seawater, 60 °C	1,200 mA cm ⁻²	100 h	[18]
Pt-Ni ₃ N@V ₂ O ₃ NiFe LDH	6 M KOH + seawater, 60 °C	1,200 mA cm ⁻²	24 h	[19]
Fe, P-NiSe ₂ NFs/CP Fe, P-NiSe ₂ NFs/CP	0.5 M KOH + seawater, 50 °C	1,100 mA cm ⁻²	200 h	[20]
Ru-Ni ₂ P/Ni ₅ P ₄ Ru-Ni ₂ P/Ni ₅ P ₄	1 M KOH + seawater, 60 °C	1,000 mA cm ⁻²	120 h	[21]
Ru/P-Fe ₃ O ₄ @IF S-N, F	1 M KOH + seawater, 60 °C	1,000 mA cm ⁻²	100 h	[22]
Pt/C Ru _{0.1} -NiFeOOH/PO ₄ ³⁻	1 M KOH + seawater, 80 °C	1,000 mA cm ⁻²	100 h	[23]
P-Os/NiFe RuO ₂ /NiFe	1 M KOH + seawater, 60 °C	600 mA cm ⁻²	100 h	[24]
Co/P-Fe ₃ O ₄ @IF Co/P-Fe ₃ O ₄ @IF	1 M KOH + seawater, 60 °C	400 mA cm ⁻²	50 h	[25]

**Figure 1.** Scheme of challenges under seawater electrolysis on anion exchange membrane-based water electrolyzer.

Membrane electrode assemblies (MEA) optimized for seawater electrolysis also offer new solutions by improving ionic selectivity and stability over extended operation^[16,32]. Modern seawater electrolysis systems utilizing MEAs are generally classified based on the electrolytes they use. Among these, the forward osmosis water electrolyzer (FOWS) integrates a desalination process that relies on a semipermeable membrane, enabling simultaneous natural seawater purification and electrolysis^[33-35]. Because the membrane isolates the anode and cathode from direct contact with seawater, the catalysts used in FOWS do not necessarily require high selectivity or corrosion resistance. However, significant challenges remain, including insufficient membrane functionality to prevent gas crossover, competitive side reactions, incomplete suppression of chloride ion diffusion into the cell, and the reverse transport of buffered species^[36].

Proton exchange membrane water electrolyzers (PEMWE) represent a promising and mature technology for large-scale seawater electrolysis^[37,38]. Nonetheless, their application is hindered by issues such as

competitive CIER against OER at the anode and the formation of insoluble precipitates at the cathode under acidic conditions. To address these challenges, catalysts for PEMWE must exhibit exceptional selectivity and stability, necessitating the use of noble metals capable of functioning in highly acidic working conditions. Additionally, cationic impurities competing with proton transport through the proton exchange membrane (PEM) and the obstruction of ion transport pathways by bacteria, microbes, or other contaminants further compromise seawater electrolysis. As an alternative, anion exchange membrane water electrolyzers (AEMWE) have gained considerable attention in recent years due to their sustainable seawater electrolysis at low costs with great performance^[39].

Unlike PEMWE, the alkaline electrolyte in AEMWE significantly mitigates competitive CIER during OER, enabling the use of abundant, low-cost materials for both the cathode and anode^[40,41]. This substitution lowers the overall system cost, making AEMWE highly appealing for commercial applications. Besides, the permselectivity of the AEM helps slow the transport of cationic impurities to the cathode, potentially reducing cathode fouling rates. The use of AEM also effectively suppresses the migration of unwanted anions such as Cl^- and Br^- , thereby decelerating the physical degradation of system components. Despite these advantages, several critical challenges remain for the industrial application of AEMWE. These include the need for advanced membranes that completely block impurity transport and the development of highly efficient and durable catalysts to ensure long-term performance under practical operating conditions.

This review provides insight into various aspects of seawater electrolysis, including key challenges, advancements in catalyst designs, and innovations in electrolyzer configurations. It highlights the latest developments that are paving the way for reliable and sustainable hydrogen production from seawater, aiming to bridge the gap between laboratory research and industrial applications.

CHLORIDE INTERFERENCE IN SEAWATER ELECTROLYSIS

Seawater electrolysis faces significant challenges due to the presence of chloride ions (Cl^-), which compete with the OER at the anode. With concentrations around 0.5 M, Cl^- ions readily adsorb onto the catalyst surface, triggering the CIER^[42]. This competition reduces hydrogen production efficiency and accelerates electrode corrosion^[43]. The initial impact of Cl^- ions on the catalyst surface involves penetrating the catalyst layer, dissolving metal components, and creating localized pits [Figure 2A]^[44]. As these pits deepen, they cause detachment of the catalytic material, compromising the electrode stability and activity. Intermediate chlorinated species formed during the process further accelerate degradation by attacking both the catalyst and the underlying substrate, significantly limiting the lifespan of electrolyzers^[45-48].

To mitigate chloride-induced degradation, several protective strategies have been developed [Figure 2B]. These include using barrier layers containing negatively charged ions to repel Cl^- ions from catalytic surfaces and reduce the adsorption on active sites. Additionally, protective coatings such as manganese oxide inhibit chloride migration through the catalyst, shielding the underlying metal substrate from chemical attack and enhancing electrode durability^[31]. These strategies aim to reduce the interaction between chloride ions and the catalyst surface, thereby improving the durability of seawater electrolyzers during long-term operation in saline environments.

To deepen our understanding of these mitigation strategies, it is critical to investigate the interactions between chloride ions and catalyst surfaces under operational conditions. Advanced characterization techniques provide invaluable insights into these mechanisms. *Ex-situ* methods, such as X-ray diffraction (XRD) and scanning electron microscopy (SEM), analyze structural and morphological changes post-electrolysis. *In-situ* techniques, including X-ray absorption near-edge structure (XANES), offer real-time

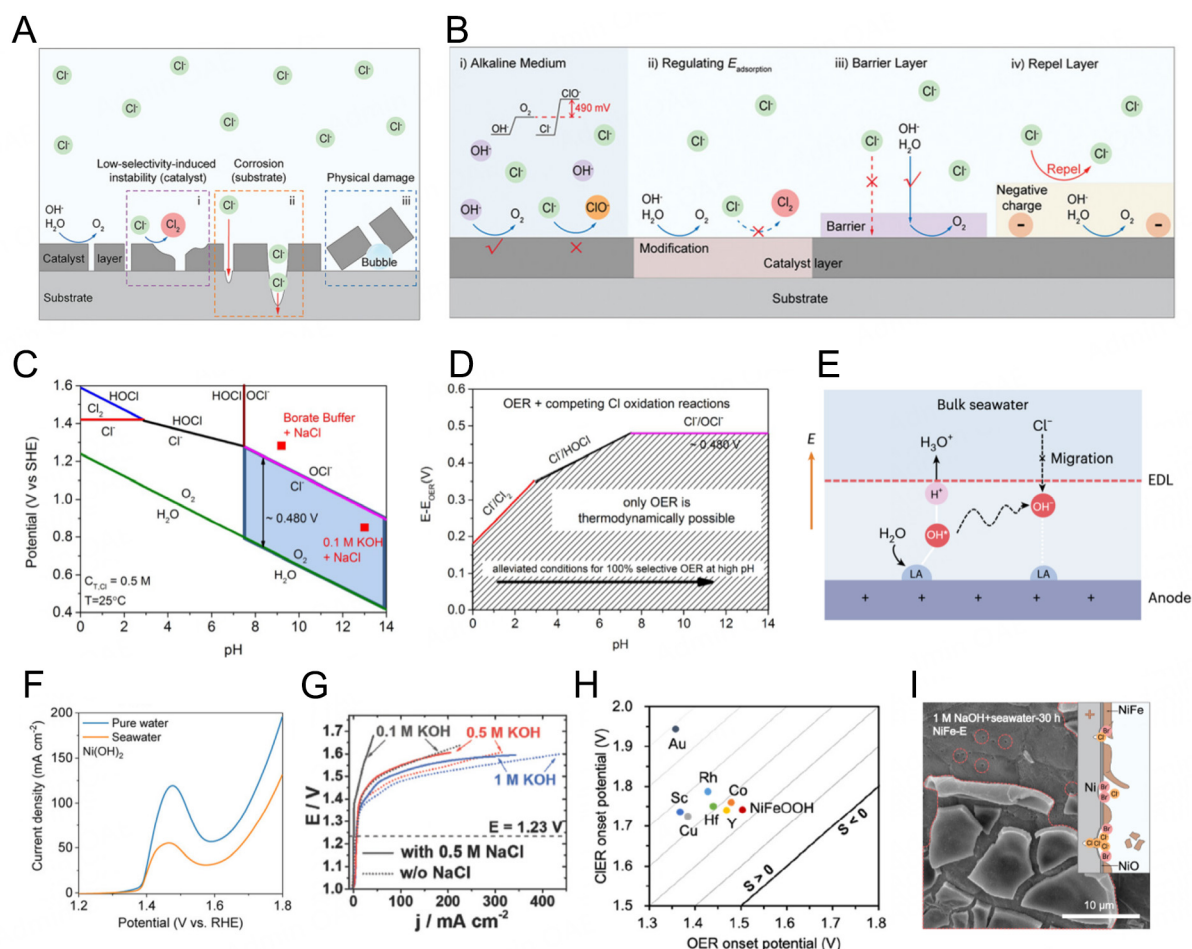


Figure 2. (A) Schematic diagram of the corrosion of the catalyst layer induced by the Cl^- ions and (B) strategies to suppress ClER and increase OER selectivity. (A and B) This figure is quoted with permission from Zhang *et al.* Copyright (2024) Wiley-VCH GmbH^[44]. (C) Pourbaix diagram for artificial seawater model and (D) Maximum allowed overpotential of OER electrolyzer catalysts to ensure 100% selective water splitting from the difference between standard electrode potentials of the three relevant chloride oxidation reactions and the OER vs. pH. (C and D) This figure is quoted with permission from Dionigi *et al.* Copyright (2016) ChemPubSoc Europe^[51]. (E) Scheme of the inhibited chlorine-related adsorption from local alkaline microenvironment generation on Lewis acid-modified anode. This figure is quoted with permission from Guo *et al.* Copyright (2023) Springer Nature^[52]. (F) Recorded LSV of OER performance of $\text{Ni}(\text{OH})_2$ under pure water and seawater conditions. This figure is quoted with permission from Liu *et al.* Copyright (2023) Wiley-VCH GmbH^[49]. (G) Polarization curves extracted from the cyclic voltammetry in different electrolytes, NiFe-LDH as anode material. This figure is quoted with permission from Dresch *et al.* Copyright (2018) Wiley-VCH GmbH^[53]. (H) Scatter plot of computed OER and ClER onset potentials. This figure is quoted with permission from Jung *et al.* Copyright (2024) American Chemical Society^[54]. (I) Corresponding SEM images of NiFe-E observed after 30 h operation in 1 M NaOH + seawater. This figure is quoted with permission from Zhang *et al.* Copyright (2023) Springer Nature^[55].

analysis of electronic and structural changes in catalysts during operation. For instance, Liu *et al.* used *in-situ* XANES to reveal that Cl^- adsorption on Fe sites in nickel-iron layered double hydroxide (NiFe LDH) induces partial reduction of Fe centers, stabilizing the Fe valence state and suppressing Fe leaching^[49]. This stabilization mitigates the loss of active sites while simultaneously promoting the oxidation of Ni centers, which enhances the OER. Furthermore, the Cl^- -induced stabilization of Ni sites was shown to improve catalytic activity by maintaining a highly oxidized and active surface, critical for sustained seawater electrolysis under alkaline conditions. These characterization techniques help address the knowledge gap between alkaline pure water and seawater electrolysis systems^[50]. Combining design strategies with advanced characterization tools provides deeper insights into the complex interactions in seawater

electrolysis and supports the development of durable and efficient catalysts for commercial applications.

The thermodynamics governing CLER and OER are heavily influenced by the pH of the electrolyte. As shown in the Pourbaix diagram [Figure 2C], the equilibrium potential for CLER increases with pH, creating a larger potential gap between CLER and OER at higher pH levels^[51]. This makes alkaline conditions (pH > 7.5) favorable for suppressing CLER, allowing OER to dominate. In acidic environments, however, the competition is more intense due to the proximity of their potential.

In acidic conditions, CLER follows the reaction: $2\text{Cl}^- \rightarrow \text{Cl}_2 + 2\text{e}^-$. This reaction occurs at approximately 1.36 V vs. the standard hydrogen electrode (SHE), close to the OER potential of 1.23 V vs. the reversible hydrogen electrode (RHE). This relatively small potential difference makes it difficult to suppress CLER in acidic media, resulting in the evolution of toxic chlorine gas. In contrast, in alkaline media, Cl^- ions prefer to react with hydroxide ions to form hypochlorite: $\text{Cl}^- + 2\text{OH}^- \rightarrow \text{ClO}^- + \text{H}_2\text{O} + 2\text{e}^-$. Although hypochlorite is less aggressive than chlorine gas, it still contributes to long-term degradation of the electrode, requiring strategies to minimize and control its formation carefully. Since the difference in potential between OER and CLER remains constant at approximately 480 mV at pH > 7.5, operating in alkaline conditions provides a crucial advantage [Figure 2D]. Operating within this window ensures that OER remains thermodynamically favored and suppresses CLER preventing the formation of corrosive hypochlorite. This operating strategy is essential for achieving stable and selective oxygen evolution under the high current densities required in commercial electrolyzers.

Electrochemical performance can also be enhanced by modulating a localized chemical environment on the electrode surface. For example, Lewis acid-modified surfaces promote water dissociation, generating excess OH^- ions near the electrode^[52]. The excess OH^- ions accumulate near the electrode and form a stable electrical double layer (EDL), which electrostatically repels Cl^- ions, preventing their adsorption on active sites [Figure 2E]. This configuration ensures that OER remains efficient, even in seawater, by blocking CLER through localized enrichment of OH^- ions.

The impact of Cl^- on the catalytic performance is further revealed through polarization and linear sweep voltammetry measurements [Figure 2F and G]^[49,53]. The measurements indicate a decrease in current densities upon the addition of NaCl, which confirms that Cl^- ions block active catalytic sites, thereby lowering OER efficiency. The reduction in catalytic performance necessitates the restriction of surface Cl^- adsorption on the electrode surfaces.

Evaluating the balance between OER activity and CLER suppression can benefit significantly from computational approaches. One such metric is the selectivity factor S , defined as the difference between computationally calculated CLER and OER overpotentials [Figure 2H]^[54]. A large positive S value indicates that the material effectively suppresses CLER, leading to high OER selectivity. Simultaneously, a low OER overpotential corresponds to enhanced catalytic activity, ensuring efficient oxygen evolution. Dopants such as Au, Sc, and Cu have shown potential to enhance conventional NiFe oxyhydroxide catalysts for seawater electrolysis by offering both high activity and effective CLER suppression, making them promising candidates for durable and efficient seawater electrolyzers.

Besides, recent studies have demonstrated that environments containing both Cl^- and Br^- ions cause detrimental corrosion under prolonged operation [Figure 2I]^[55]. In NaCl-containing electrolytes, the localized deep pits form in weak areas of the catalyst layer, leading to significant degradation. In NaBr solutions, however, the corrosion produces wider but shallower pits, indicating a different degradation

mechanism. The mixed corrosion patterns observed in seawater electrolysis highlight the complex interplay of halide ions. While abundant Cl^- ions initiate localized corrosion, Br^- ions accelerate the degradation process even at low concentrations through their oxidative activity. These findings emphasize the importance of addressing both Cl^- and Br^- ions in catalyst design and electrolyte management to mitigate halide-induced corrosion and ensure long-term stability.

STRATEGIES TO MITIGATE CHLORIDE-INDUCED CHALLENGES

Chloride ions present a significant challenge to seawater electrolysis by competing with OER, triggering ClER, and promoting corrosion. However, advances in catalyst design, the use of protective layers, alkaline operating strategies, and rational catalyst designs are steadily improving system performance and essential steps toward developing durable efficient seawater electrolyzers^[56,57]. Recent studies have demonstrated that the stability of anodes in seawater electrolysis can be significantly improved through the strategic design of catalysts that incorporate protective anti-chloride corrosion layers^[58,59]. One effective approach is to create surfaces enriched with anions, which electrostatically repel chloride ions. However, this strategy introduces a challenge that repelling Cl^- can also hinder the adsorption of hydroxide ions (OH^-), which are crucial for efficient OER. As such, researchers have focused on innovative designs that balance these competing interactions.

In one approach, RuMoNi nanorods were developed using a two-step synthesis involving hydrothermal treatment and electrochemical activation, which resulted in the *in-situ* formation of MoO_4^{2-} on the surface [Figure 3A]^[16]. These MoO_4^{2-} anions effectively repel Cl^- ions, enhancing the electrode's corrosion resistance. The RuMoNi electrocatalyst achieved nearly 100% OER selectivity in seawater, maintaining stable operation for over 3,000 h at a current density of 500 mA cm^{-2} , with minimal degradation ($0.64 \mu\text{V h}^{-1}$). Even in electrolytes with three times the NaCl concentration of seawater, the nanorod structure remained intact, underscoring its robustness. Furthermore, ultraviolet-visible (UV-vis) spectroscopy confirmed the absence of hypochlorite, a byproduct of ClER, demonstrating excellent OER selectivity and corrosion resistance [Figure 3B]. The success of the RuMoNi catalyst lies in the strong electrostatic repulsion between MoO_4^{2-} and Cl^- , while the hydrogen bonding between Ni_4Mo and OH^- mitigates the negative effects of OH^- repulsion, maintaining OER kinetics.

Another study by Gong *et al.* introduced a core-shell structure consisting of NiFe alloys encapsulated within defective graphene layers (NiFe@DG), synthesized via a microwave thermal shock process [Figure 3C]^[46]. This design leverages the graphene shell to create a built-in electric field that repels Cl^- ions while permitting OH^- transport, ensuring high OER selectivity. The NiFe@DG catalyst maintained stable performance for over 2,000 h with only a 1% reduction in OER activity in alkaline seawater. In contrast, the oxidation peak of Ni observed in NiFe/G vanished after stability tests due to metal dissolution, while the peak remained intact for NiFe@DG, indicating enhanced corrosion resistance. X-ray photoelectron spectroscopy (XPS) analysis of the Cl 2p spectrum further revealed no detectable chloride species on NiFe@DG, while significant peaks were observed for NiFe/G, confirming the effectiveness of the graphene confinement in preventing chloride-induced corrosion.

Recently, Cr dopants were introduced on NiFe catalysts by immersing NiFe LDH-coated nickel foam (NF) in a sodium chromate solution, where OH^- ions preferentially adsorbed over Cl^- ^[60]. This catalyst design incorporated both nanosized Cr_2O_3 and CrO_4^{2-} anions, which acted as Lewis acid sites, enriching the local OH^- concentration and electrostatically repelling Cl^- ions [Figure 3D]. These features fostered a surface with selective OH^- adsorption, which is essential for efficient OER. The Cr-modified NiFe LDH catalyst demonstrated remarkable durability, sustaining continuous electrolysis for over 2,400 h at current densities

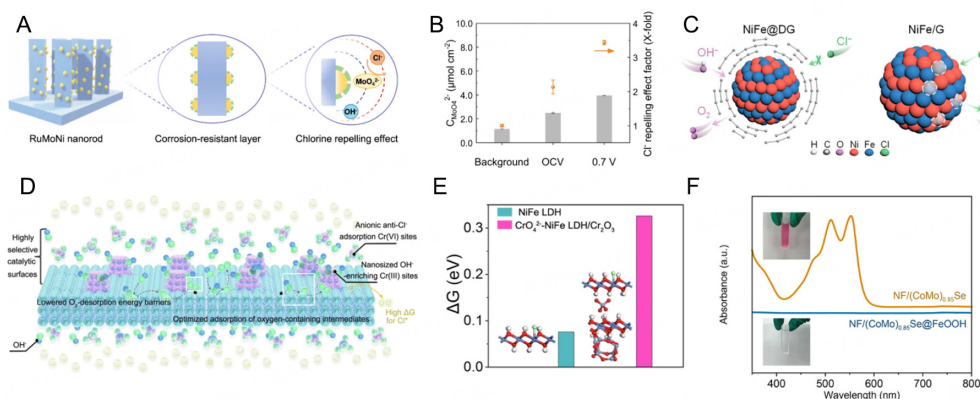


Figure 3. (A) Design strategy of the RuMoNi catalyst. The light blue bar, yellow semicircle, and green dotted lines represent nanorod substrate, catalytic active sites, and corrosion-resistant layer, respectively. (B) The adsorbed MoO_4^{2-} concentration on carbon paper (background) and RuMoNi normalized by electrode area and corresponding Cl⁻ repelling effect factors. (A and B) This figure is quoted with permission from Liu *et al.* Copyright (2023) Springer Nature^[61]. (C) Schematic illustration of the mechanism of the improved durability for the NiFe nanoalloys encapsulated within defective graphene layers (NiFe@DG) compared to the uncoated NiFe nanoalloys supported on graphene (NiFe/G). This figure is quoted with permission from Fei *et al.* Copyright (2023) Americal Chemical Society^[46]. (D) Schematic illustrating the concept of creating an anion-rich catalytic surface on CrO_4^{2-} -NiFe LDH/ Cr_2O_3 that selectively repel Cl⁻ and enrich OH⁻. (E) Free energy calculations for the adsorption of Cl⁻ with atomic structures. (D and E) This figure is quoted with permission from Tang *et al.* Copyright (2024) Springer Nature^[60]. (F) UV-vis absorption spectra for the detection of hypochlorite species in the electrolyte with the inset showing optical photos of the pH-adjusted electrolyte after adding DPD. This figure is quoted with permission from Yang *et al.* Copyright (2023) Americal Chemical Society^[61].

of 1,000 to 2,000 mA cm^{-2} in alkaline seawater. UV-vis results confirmed that the Cr-modified catalyst produced minimal active chlorine even after 1,000 h, while the unmodified NiFe LDH generated significant chlorine levels within 50 h of operation. The enhanced corrosion resistance is attributed to the higher adsorption energy of OH⁻ over Cl⁻ on the Cr-modified catalyst surface [Figure 3E].

Yang *et al.* also proposed a multilayered heterostructure featuring an amorphous FeOOH overlayer on crystalline Mo-doped $\text{Co}_{0.85}\text{Se}$ nanosheet arrays, aligned on NF ($\text{NF}/(\text{CoMo})_{0.85}\text{Se@FeOOH}$)^[61]. This three-step synthesis involved hydrothermal reactions followed by an interfacial reaction to create a robust core-shell structure. The FeOOH shell, combined with *in-situ* formed polyatomic anions such as MoO_x^{n-} or SeO_x^{n-} , provided a permselective barrier that prevented Cl⁻ penetration. This structure exhibited stable performance for over 160 h at a current density of 300 mA cm^{-2} in alkaline seawater. Even in an electrolyte containing four times the NaCl concentration of seawater (1 M KOH + 2 M NaCl), the catalysts maintained initial catalytic performance after 75 h, significantly outperforming its uncoated counterpart, which failed after 9 h. The absence of hypochlorite was confirmed indicating effective Cl⁻ repulsion by the FeOOH-coated catalyst [Figure 3F].

These examples highlight the effectiveness of innovative material designs in mitigating the challenges posed by Cl⁻ in seawater electrolysis. By carefully tuning catalyst surfaces, introducing protective layers, and controlling operating conditions, researchers have made significant progress in developing durable, corrosion-resistant anodes. However, further research is needed to refine these strategies and scale them for commercial applications. With optimized catalysts and robust system design, seawater electrolysis has the potential to become a scalable and sustainable solution for green hydrogen production, leveraging the vast availability of seawater as a resource.

IMPACT OF ELEVATED PH ON PRECIPITATE FORMATION IN SEAWATER ELECTROLYSIS

A persistent challenge in seawater electrolysis is the accumulation of Mg^{2+} and Ca^{2+} ions on the cathode, which block active sites, increase voltage losses, and hinder hydrogen production. Over time, these precipitates form hydroxides and carbonates, reducing Faradaic efficiency and damaging the electrode. Unlike indirect seawater electrolysis, direct seawater splitting utilizes seawater without pretreatment^[62]. The formation of precipitates such as magnesium hydroxide [$\text{Mg}(\text{OH})_2$] and calcium carbonate (CaCO_3) poses a significant threat to the efficiency and longevity of the electrolyzers used in this process^[63–66]. During the HER, which occurs at the cathode, the local pH near the electrode increases due to the consumption of protons (H^+) and the generation of hydroxide ions (OH^-). This localized pH increase promotes the precipitation of impure cations such as Mg^{2+} and Ca^{2+} , which are present in unfiltered seawater^[67–70]. These cations form insoluble compounds on the cathode, causing blockage and significantly hindering the overall reaction. The formation of blocking precipitates in seawater electrolysis is closely tied to the local electrochemical environment at the cathode. As hydrogen evolves, the depletion of protons and the accumulation of hydroxide ions at the electrode surface causes the local pH to rise, particularly in the near-neutral pH range of seawater (around pH 8). This local alkaline environment triggers the precipitation of Mg^{2+} and Ca^{2+} , which form $\text{Mg}(\text{OH})_2$ and CaCO_3 , respectively^[71–73].

Seawater contains approximately 1,300 ppm of Mg^{2+} which precipitates as $\text{Mg}(\text{OH})_2$ when the local pH exceeds 9.3. The deposition of $\text{Mg}(\text{OH})_2$ on the cathode forms an insulating layer that blocks active sites of catalysts, significantly reducing efficiency and increasing the overpotential. Additionally, seawater contains around 400 ppm of Ca^{2+} which primarily precipitates as CaCO_3 in the presence of carbonate ions (CO_3^{2-}) formed by dissolved carbon dioxide^[74]. These precipitates also physically block the cathode, further reducing the efficiency of HER.

These two precipitations present a significant challenge to the long-term stability of direct seawater electrolysis systems. Continuous operation leads to the accumulation of these deposits, eventually necessitating a shutdown for the elimination of fragments or replacement of cell components.

In neutral seawater (pH ~8), the consumption of H^+ ions during HER causes the local pH to rise, often exceeding the solubility limits of $\text{Mg}(\text{OH})_2$ and CaCO_3 while increasing the amounts of deposits. At the industrial high current density, the formation of these precipitates is more pronounced. In addition to local pH effects, the lifespan of the system is influenced by the interplay between the cathode and anode. While HER increases the local pH of the cathode, OER decreases the local pH of the anode due to proton generation. This pH gradient across the electrodes can intensify the precipitation on the cathode while promoting corrosion at the anode due to the acidic environment. Numerous strategies have been developed to address the challenge of precipitation during the electrolysis, focusing on catalyst design^[75,76], membrane technologies^[77–79], and electrolyte management^[80]. The combinations of these solutions mitigate the detrimental effects of precipitate accumulation and contribute to the practical application of direct seawater electrolysis.

MITIGATION STRATEGIES FOR PRECIPITATION AND PH-RELATED CHALLENGES

To address the challenges posed by precipitate accumulation, researchers have explored catalyst design, membrane technologies, and electrolyte management. Among these, the development of anti-precipitation catalysts has shown significant promise for enhancing performance in seawater electrolysis. Kang *et al.* designed a hydrophobic nanobundle-structured cathode that prevents impurity precipitation^[64]. The electrode was developed by anodizing Cu mesh to form nanobundle arrays, followed by hydrophobic

surface treatment with dodecanethiol. The HER primarily occurs at the nanobundle tips, where active sites are densely concentrated. The generated H_2 gas aggregates to bubble and creates a physical barrier on the cathode surface, preventing contact with precipitate-forming species such as H_2O , Ca^{2+} , and CO_3^{2-} . Due to the structural characteristics of the nanobundles, precipitates only adhere loosely at the tips and are automatically removed by the bursting of hydrogen bubbles, leading to efficient self-cleaning of the electrode.

In another approach, Liang *et al.* modified the surface environment of a commercial Pt/C catalyst by mixing it with 1,8-bis(dimethylamino)naphthalene (DMAN), which acts as a proton sponge to repel Mg^{2+} and Ca^{2+} ions^[81]. The seawater electrolysis with this modified catalyst not only prevents the deterioration in efficiency caused by physical contamination but also offers an environmentally friendly synthetic route of $\text{Mg}(\text{OH})_2$. The addition of DMAN induces positive charges on the Pt/C cathode, introducing a repelling against Mg^{2+} and Ca^{2+} cations, thereby suppressing the formation of precipitates.

Zhao *et al.* developed an anti-precipitation HER catalyst by modifying Pt nanoparticles on carbon nanotube (Pt/CNT) with molecular metal chalcogenide complexes. The catalyst is designed to block the interaction of Mg^{2+} and Ca^{2+} ions with the active sites on the catalyst during high-current density electrolysis^[82]. The Pt/CNT-200 effectively prevents the deposition of insoluble precipitates on the cathode surface, maintaining high catalytic activity and stability in seawater electrolysis. The anti-precipitation properties of the catalyst are rooted in the coordination compounds formed by the molecular metal chalcogenides and the cations (Mg^{2+} and Ca^{2+}). These formations hinder the bonding of metal cations with hydroxide ions. The products remain below the solubility constant for $\text{Mg}(\text{OH})_2$ and $\text{Ca}(\text{OH})_2$, effectively preventing the formation of insoluble precipitates on the catalyst.

Guo *et al.* adjusted the local reaction environment at the cathode to inhibit unwanted precipitation by using a Lewis acid surface with Cr_2O_3 -modified CoO_x catalysts [Figure 4A]^[52]. The catalyst enhances HER activity while preventing the precipitations. Even after 2 h of continuous HER operation, the pH of bulk seawater in Cr_2O_3 - CoO_x remains below 9.3, the point at which precipitation occurs, while precipitation occurs in the bulk seawater of CoO_x [Figure 4B]. The introduction of a Cr_2O_3 layer to the CoO_x catalyst creates a hard Lewis acid surface that binds strongly to OH^- . This layer restricts the interaction of free OH^- ions with Mg^{2+} and Ca^{2+} [Figure 4C]. By limiting the diffusion of OH^- into the bulk electrolyte, the Cr_2O_3 layer prevents the local pH from significantly rising, which is crucial for preventing the formation of $\text{Mg}(\text{OH})_2$ and CaCO_3 . The cell utilizing the Cr_2O_3 - CoO_x electrodes achieved current densities of 100 mA cm^{-2} at 1.89 V, with stable operation for over 100 h at 500 mA cm^{-2} in natural seawater. XRD confirmed no significant precipitates formed on the Cr_2O_3 - CoO_x cathode compared to the unmodified cathode, where $\text{Mg}(\text{OH})_2$ was observed at a higher pH [Figure 4D]. The modified cathode was applied in a flow-type electrolyzer, achieving industrial-level hydrogen production (1.0 A cm^{-2} at 1.87 V in 60°C of electrolyte). The system ensured stable operation for over 100 h, maintaining high Faradaic efficiency ($\sim 100\%$) in 25°C natural seawater, making it suitable for practical hydrogen production from seawater without complex desalination or chemical pretreatment.

Li *et al.* introduced a Cu-modulated ruthenium cluster on a porous carbon matrix ($\text{Cu@Ru}_{\text{nc}}\text{-C}$), synthesized from a polyhedral metal-organic precursor via thermal annealing and acid etching^[83]. This material serves as an effective proton supply and anti-poisoning cathode material for superior direct hydrogen production from seawater. The operational durability of both $\text{Cu@Ru}_{\text{nc}}\text{-C}$ and $\text{Ru}_{\text{nc}}\text{-C}$ was assessed under seawater and alkaline seawater conditions. The $\text{Cu@Ru}_{\text{nc}}\text{-C}$ exhibited negligible activity loss, whereas $\text{Ru}_{\text{nc}}\text{-C}$ experienced a rapid decline in activity in seawater. Mechanistic investigation revealed that the ruthenium cathode featuring Cu@Ru_{nc} pair sites provides a low oxophilic and rapid proton-transferring

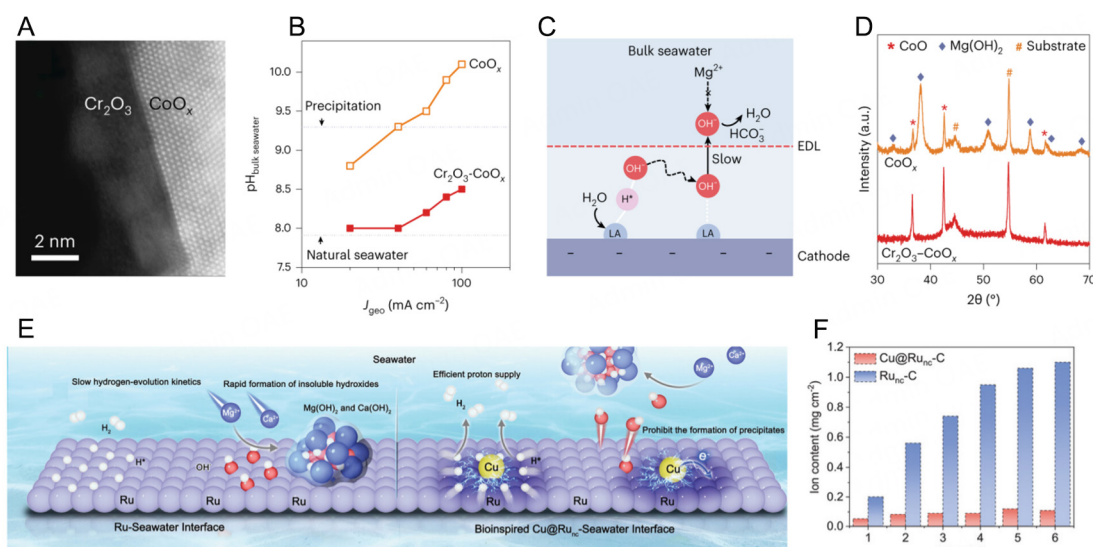


Figure 4. (A) TEM image of the interface of as prepared $\text{Cr}_2\text{O}_3\text{-CoO}_x$ cathodes (B) pH values of bulk seawater around CoO_x and $\text{Cr}_2\text{O}_3\text{-CoO}_x$ cathodes. (C) Schematic illustration of local alkaline microenvironment generation on Lewis acid-modified cathode, which facilitates HER and prevents precipitate formation. (D) XRD spectra of CoO_x and $\text{Cr}_2\text{O}_3\text{-CoO}_x$ cathodes after operating at 100 mA cm^{-2} for 2 h. This figure is quoted with permission from Guo *et al.* Copyright (2023) Springer Nature^[52]. (E) Comparison of Ru-seawater interface and bioinspired Cu@Ru_{nc} -seawater interface for seawater hydrogen production. (F) Ion contents of Mg and Ca in seawater of different catalysts after chronopotentiometry tests. (E and F) This figure is quoted with permission from Li *et al.* Copyright (2024) Wiley-VCH GmbH^[83].

local reaction environments, which inhibits the formation of insoluble precipitates and ensures efficient proton supply at the electrode-seawater interface [Figure 4E]. XPS analyses quantitatively confirmed the concentrations of Mg and Ca ions after the seawater HER. The $\text{Cu@Ru}_{\text{nc}}\text{-C}$ exhibited significantly lower concentrations of Mg and Ca ions compared to $\text{Ru}_{\text{nc}}\text{-C}$, which can be attributed to the rapid release of OH^- from the electrode-seawater interface, thereby limiting the generation of insoluble precipitates [Figure 4F]. SEM images of both $\text{Cu@Ru}_{\text{nc}}\text{-C}$ and $\text{Ru}_{\text{nc}}\text{-C}$ post-HER test demonstrated that the $\text{Ru}_{\text{nc}}\text{-C}$ was covered with abundant Mg and Ca precipitate-based nanosheets, while only minimal hydroxide precipitates were observed around the $\text{Cu@Ru}_{\text{nc}}\text{-C}$ catalyst. This observation suggests that the rapid OH^- release process in $\text{Cu@Ru}_{\text{nc}}\text{-C}$ effectively inhibits the growth of hydroxide crystals, establishing it as an anti-poisoning cathode suitable for long-term seawater splitting. These findings further indicate that the unique Cu@Ru_{nc} pair sites significantly modulate the microenvironments at the electrode interface, alleviating OH^- occupation on Ru sites due to their weak binding, thus preventing the formation of hydroxide precipitates and restricting blockage of Ru sites by insoluble precipitates.

The precipitation of Mg(OH)_2 and Ca(OH)_2 at the cathode blocks the catalytic active sites, and this issue becomes more pronounced at high current operation. Bubble removal from the cathode surface is one potential approach for stable long-term operation under high current conditions. To address the precipitation of Mg^{2+} and Ca^{2+} ions at the cathode that blocks the catalytic active sites, Liang *et al.* developed a novel microscopic bubble/precipitate traffic system (MBPTS), utilizing NiCoP (NCP) nanostructures on a pinewood-derived carbon (PC) framework^[84]. This three-dimensional honeycomb-like architecture offers a dual benefit: promoting the release of H_2 bubbles while actively repelling Mg/Ca precipitates through dynamic airflow [Figure 5A]. The PC framework, produced through pyrolysis, offers a lightweight, self-supporting structure with interconnected channels that promote ion and gas flow, ensuring smooth hydrogen evolution and mitigating precipitate formation.

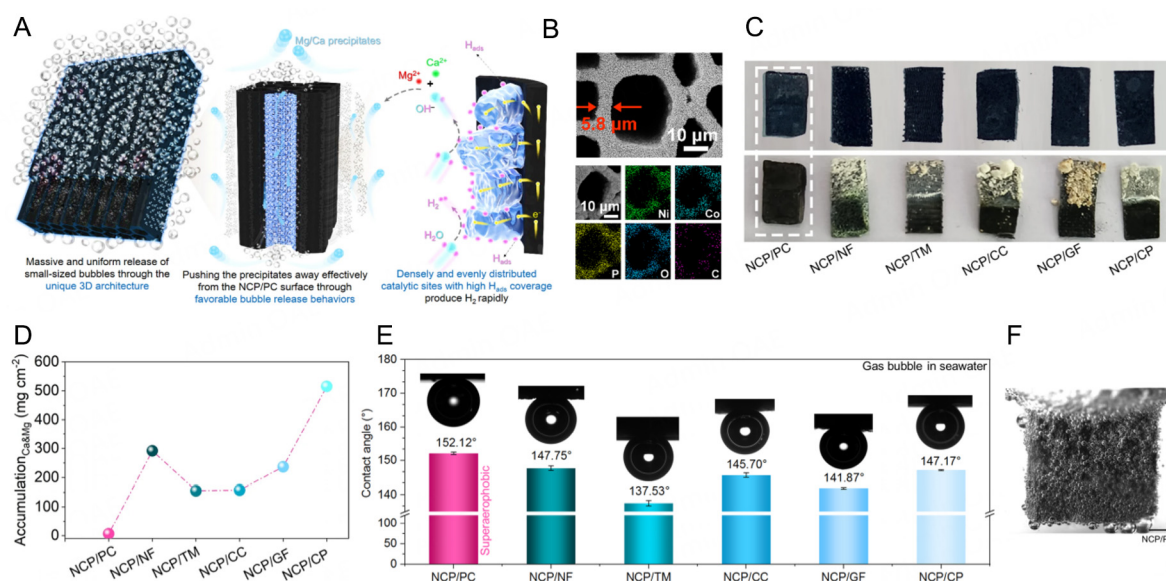


Figure 5. (A) Schematics of efficient traffic of bubbles and insoluble precipitates on/in the NiCoP-decorated pinewood-derived carbon (NCP/PC). (B) Cross-sectional view SEM image and elemental EDS of PC. (C) Photographs of the various cathodes after the long-term electrochemical natural seawater reduction testing and (D) the accumulation value of Mg and Ca. (F) Gaseous H_2 release behaviors on NCP/CP at the j of magnitude of 500 mA cm^{-2} (E) Underwater gas-bubble contact angle data. (A-F) This figure is quoted with permission from Liang et al. Copyright (2024) Springer Nature^[84].

The NCP nanostructures grow uniformly along the microchannels without blocking them [Figure 5B]. These channels allow H_2 bubbles to escape efficiently, generating localized airflow that repels Mg^{2+} and Ca^{2+} ions before they can form deposits. The small, evenly distributed bubbles detach at optimal velocities, maintaining active catalytic sites free from blockage. This dynamic bubble management system enables long-term stable operation, even under high current densities, by continuously clearing precipitates from the electrode surface.

Performance comparisons with other NCP-based cathodes, such as those supported on carbon cloth (CC), NF, and titanium mesh (TM), demonstrated the superior anti-precipitation properties of NCP decorated PC (NCP/PC). As shown in Figure 5C, only the NCP/PC cathode remained clean after extended operation, while others were heavily coated with Mg^{2+}/Ca^{2+} precipitates. XRD analysis further confirmed the absence of significant precipitate peaks on NCP/PC, highlighting its resistance to fouling. The anti-precipitation performance was quantified using the accumulation amount of Mg and Ca ions, which measures the total content of Mg and Ca normalized to the electrode area [Figure 5D]. NCP/PC exhibited minimal accumulation ($\sim 6 \text{ mg cm}^{-2}$), far less than the other cathodes, which accumulated 20–80 times more deposits. This performance is attributed to the ability of the MBPTS to prevent ions from settling on the electrode surface through continuous gas-driven clearing.

In addition to its anti-precipitation properties, NCP/PC excels in gas release management. NCP/PC exhibited the largest air contact angle, making it highly hydrophilic and aerophobic [Figure 5E]. This characteristic ensures that bubbles detach smoothly, further preventing clogging by precipitates and promoting continuous hydrogen evolution. The flow-type electrolyzer test demonstrated that the NCP/PC cathode maintained a stable current density of 500 mA cm^{-2} over 150 h in untreated seawater, achieving nearly 100% Faradaic efficiency for hydrogen production. In more demanding tests at 1 A cm^{-2} , the system operated for over 1,000 h with minimal voltage decay. The uniform distribution of H_2 bubbles on the NCP/

PC cathode plays a crucial role in maintaining performance by preventing localized fouling [Figure 5F]. This dynamic bubble-precipitate management system ensures that active sites remain unobstructed, even under high current densities, enhancing both stability and efficiency.

Meanwhile, the flow of the electrolyte not only physically removes precipitates but also suppresses their formation. Liang *et al.* mitigated the degradation caused by electrode blockage through several techniques that utilize fluid flow^[81]. They employed an external flow of electrolytes to disrupt the pH gradient near the cathode. By using an external flow, the local OH^- rise of the cathode is relieved, reducing the formation of precipitates. This flow also helps carry away any small particles of precipitate, reducing their accumulation on the cathode surface. This cathode design features a porous structure that facilitates the release of hydrogen gas bubbles. These bubbles create upward flows that mechanically remove the precipitates that form near the cathode. This dynamic movement of gas and liquid helps maintain a clean electrode surface, preventing significant deposition of $\text{Mg}(\text{OH})_2$ or CaCO_3 . Thus, liquid and gas strategies allow for continuous operation without the need for external cleaning processes, making cathodes highly suitable for long-term seawater electrolysis operation.

Various studies focused on the systematic approach of seawater electrolysis such as modifying the reaction environment, optimizing electrolytes, and incorporating advanced membranes to prevent fouling have been actively developed. Recently, a bioelectrochemical precipitation system (BES) was adopted to obstruct the formation of precipitates and to generate OH^- at the cathode through electrochemical reactions^[85]. The intentional production of OH^- enables selective precipitation of scale-forming ions, preventing them from causing blockage on the electrodes or membranes. In addition, they employed two different buffer solutions, phosphate buffer solution (PBS) and piperazine-N,N'-bis(2-ethanesulfonic acid) (PIPES), to enhance the removal efficiency of Ca^{2+} and Mg^{2+} . In PBS, phosphate ions transferred from the anode to the cathode react with Ca^{2+} to form calcium phosphate, further reducing the amount of free Ca^{2+} ions that can form scale. This buffer-based strategy aids in efficient ion removal and prevents large-scale precipitation on the electrode surface. Han *et al.* impede precipitate formation by leveraging synergistic acidification via inorganic precipitation and proton flux from a bipolar membrane (BPM)^[57]. A BPM was utilized as a separator between the cathode and anode compartments. When a reverse bias was applied, the BPM dissociated water into H^+ and OH^- , with H^+ migrating toward the cathode. This proton flux helped acidify the catholyte, thereby preventing the local pH from rising too high during the HER, avoiding the risk of precipitation. Furthermore, they exploited the natural precipitation of $\text{Mg}(\text{OH})_2$ to trap excess OH^- generated by the HER. Mg^{2+} ions in seawater have a very low solubility, meaning they easily form precipitates in the presence of OH^- . By allowing controlled precipitation, hydroxide ions were effectively removed from the local environment, avoiding a significant pH rise.

Ren *et al.* introduced the dual-cation exchange membrane (CEM) and circulatory electrolyte design to ensure long-term operation of HER from cathodic contamination^[86]. The electrolyzer utilizes a CEM system that allows the selective transport of monovalent ions, such as Na^+ or K^+ , while blocking divalent ions such as Mg^{2+} and Ca^{2+} . By separating seawater from the concentrated alkaline electrolyte using CEMs, this setup prevents the accumulation of harmful precipitates at the cathode, thus avoiding the blockage of active sites and degradation of performance. In addition, the system involves the continuous circulation of concentrated alkaline electrolytes in both the cathode and anode chambers. This circulatory design maintains ionic concentration and pH balance between the two chambers, ensuring a stable transmembrane concentration gradient. This pH gradient drives efficient water migration from the seawater to the electrolyte, further preventing local pH increases at the cathode, which typically leads to precipitation. These strategies allowed for efficient and stable hydrogen production from seawater over long periods without the

need for additional chemicals or complex pretreatment processes.

PRACTICAL APPLICATION OF MEA-BASED SEAWATER ELECTROLYZERS

Recent research has made significant strides in developing MEA systems optimized for seawater electrolysis. These efforts focus on overcoming challenges such as ionic contamination, corrosion, fouling, and the high energy requirements associated with conventional OER. To address these limitations, innovative approaches have explored optimized electrolyte configurations^[87], alternative oxidation reactions such as hydrazine oxidation reaction (HzOR)^[88,89], and advanced membranes^[77], all aimed at improving system efficiency and durability.

One promising design involves a sodium-ion-conducted asymmetric electrolyzer, which uses NaCl as the catholyte and NaOH as the anolyte. This configuration creates a stable ionic environment that minimizes chloride migration and reduces the risk of corrosion at the electrodes [Figure 6A]^[87]. The selective transport of sodium ions through the membrane helps maintain stable pH conditions while minimizing chloride buildup, a key factor in enhancing system stability. Performance comparisons between symmetric NaOH electrolytes and the asymmetric NaCl/NaOH setup show that the latter achieves the same 100 mA cm⁻² current density at a lower voltage, making it more energy-efficient [Figure 6B]. Such efficiency improvements are critical for practical applications where every volt reduction contributes to significant energy savings. Further demonstrating the robustness of this design, the asymmetric system maintains 400 mA cm⁻² at 1.66 V without noticeable voltage drift, ensuring stable operation even under high current densities [Figure 6C].

However, even with these innovations, the competition between OER and ClER remains a key challenge. While OER is generally favored at moderate voltages, increasing the current density requires higher applied voltages, which can exceed the OER threshold by more than 0.48 V. This makes ClER thermodynamically favorable, leading to the evolution of chlorine gas and compromising system selectivity by causing electrode degradation [Figure 6D]. To avoid these issues, researchers have replaced OER with HzOR, which operates at a much lower potential of -0.33 V vs. RHE^[89]. This alternative reaction ensures that even under high current densities, the system avoids chlorine formation, enhancing both safety and stability [Figure 6E].

In addition, HzOR requires significantly less energy input than OER, improving overall efficiency. The use of hydrazine as the anolyte provides another important advantage. Hydrazine is commonly used in various industrial applications, including power plants and chemical manufacturing, and improper disposal can pose serious environmental risks. Incorporating hydrazine wastewater into seawater electrolysis offers a sustainable solution by simultaneously producing hydrogen and addressing pollutant remediation. The scalability of this approach is demonstrated in renewable energy-powered hybrid seawater electrolyzer (HSE) systems, designed to operate with seawater and industrial hydrazine sewage as feeds. Coastal regions with abundant solar and wind resources offer ideal conditions for deploying such systems, combining hydrogen production with wastewater treatment to maximize resource efficiency [Figure 6F].

Comparative studies between HSE and conventional alkaline seawater electrolyzers (ASEs) show that HSE systems achieve similar current densities at significantly lower voltages. While ASEs typically operate at 1.8–2.4 V to achieve practical current densities, HSE systems achieve the same performance at voltages below 1.15 V [Figure 6G]. This reduction in energy consumption is critical for industrial applications, as lower operating costs enhance the economic feasibility of the technology. The long-term stability of the hybrid system is equally important for practical application. Durability tests at 500 mA cm⁻² show that the system maintains stable performance for more than 140 h with minimal degradation [Figure 6H]. In

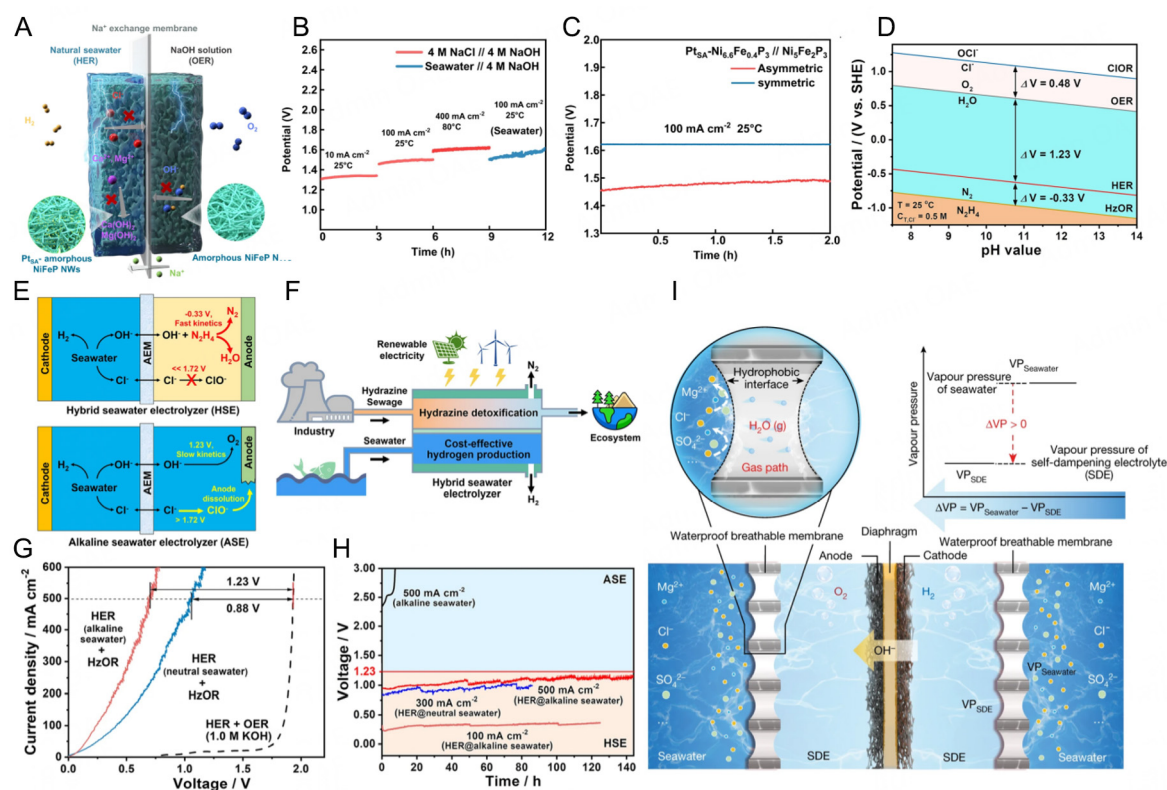


Figure 6. (A) Schematic of an asymmetric electrolyzer using NaCl and NaOH as catholyte and anolyte, respectively. (B) Voltage-current relationship comparison between symmetric and asymmetric electrolyte configurations and (C) the long-term performance of the asymmetric electrolyzer. (A-C) This figure is quoted with permission from Shi et al. Copyright (2023) Springer Nature^[87]. (D) Pourbaix diagram illustrating the competition between OER, ClOR, and HzOR. (E) Comparison of different anode behavior of HSE and ASE. (F) Schematic of a renewable energy-powered HSE system utilizing seawater and industrial hydrazine wastewater as feeds. (G) Efficiency comparison of various types of HSE and ASE and (H) stability comparison under high current densities. (D-H) This figure is quoted with permission from Sun et al. Copyright (2021) Springer Nature^[89]. (I) Membrane-assisted electrolyzer design featuring a breathable, waterproof membrane that allows water vapor transport while preventing ionic contamination. (I) This figure is quoted with permission from Xie et al. Copyright (2022) Springer Nature^[77].

contrast, ASEs experience rapid degradation due to ClER, highlighting the importance of chloride-free operation to ensure the longevity of seawater electrolyzers. The ability of HSE systems to sustain high current densities with minimal performance loss demonstrates their robustness for industrial-scale hydrogen production.

The concept of integrating hybrid oxidation reactions to improve system efficiency is also explored through a sulfon oxidation reaction (SOR)-based seawater electrolyzer^[88]. This design utilizes a needle-like Co₃S₄ catalyst grown on NF, which enhances local electric fields and accelerates the SOR kinetics. By converting harmful sulfide contaminants into sulfur byproducts, this system addresses both environmental remediation and hydrogen production needs. With stable operation for over 500 h at 100 mA cm⁻², the SOR-based electrolyzer demonstrates energy-efficient hydrogen generation without triggering ClER. Such advancements align with the broader goal of developing cleaner and more sustainable electrolysis systems.

Another critical aspect of seawater electrolysis is the prevention of fouling and ionic contamination, which can impair catalytic activity over time. To address this issue, researchers have developed advanced membranes that are both waterproof and breathable, allowing water vapor to pass through while blocking

contaminants^[77]. These membranes maintain the separation between seawater and the electrodes, preventing fouling and preserving catalytic performance throughout extended operation [Figure 6I]. Long-term testing demonstrated that the membrane-based system can operate continuously at 250 mA cm^{-2} for over 3,200 h without significant performance loss, underscoring its suitability for large-scale applications. This membrane design minimizes maintenance requirements and ensures stable gas release, making it highly practical for continuous hydrogen production in industrial environments.

These advances represent significant progress toward the practical implementation of seawater electrolysis. By adopting optimized electrolyte configurations, introducing alternative oxidation reactions such as HzOR and SOR, and utilizing advanced membranes to prevent fouling, these systems overcome the key challenges associated with conventional seawater electrolyzers and become essential components of the green hydrogen economy.

CONCLUSION AND OUTLOOK

Seawater electrolysis is a promising approach for sustainable hydrogen production, utilizing abundant seawater to meet future energy demands. However, several challenges remain, including ClER, electrode degradation, fouling, and ionic contamination. These obstacles limit system efficiency, durability, and scalability, making commercial deployment difficult. Enhancing OER selectivity over ClER is essential for improving both performance and stability. Researchers have made progress by promoting OH^- -rich microenvironments, applying barrier and repellent layers, and modifying catalyst surfaces to reduce ClER activity. Computational studies have also identified dopants such as gold, scandium, and copper, which improve catalytic performance and selectivity in saline environments. Although these developments offer promising solutions, localized corrosion at high current densities remains a concern, emphasizing the need for further improvements in catalyst design and electrolyte management.

The accumulation of magnesium and calcium precipitates at the cathode creates additional challenges by blocking active sites and reducing Faradaic efficiency. Innovations in electrode design, such as hydrophobic nanostructures, proton-absorbing coatings, and molecular metal complexes, prevent precipitate buildup and ensure uninterrupted hydrogen evolution. These advances highlight the importance of material engineering in achieving the long-term stability necessary for practical seawater electrolyzers.

The introduction of HzOR has significantly improved system efficiency by offering an alternative to OER. Since HzOR operates at much lower voltages, it eliminates the risk of ClER while reducing energy consumption. The use of industrial hydrazine wastewater as the anolyte further enhances the system by reducing operational costs and addressing environmental concerns through pollutant remediation. This dual-function approach aligns hydrogen production with sustainability goals, demonstrating the versatility of HSEs.

Seawater electrolysis enables sustainable hydrogen production and offers opportunities for recovering valuable resources such as lithium. Recent studies have demonstrated methods to simultaneously extract lithium during electrolysis using advanced systems, such as a solar-powered setup with a solid-state electrolyte. Pulsed electrochemical intercalation techniques have also demonstrated high selectivity for lithium over sodium in seawater, highlighting the potential for integrated hydrogen production and resource recovery.

However, seawater electrolysis faces challenges from various impurities beyond chloride, magnesium, and calcium ions. Heavy metal ions, such as copper and zinc, can deposit on the electrode, blocking active sites and forming passivating layers. Organic contaminants adsorb onto the electrode surface, hindering reaction kinetics, while sulfides can degrade catalyst performance by forming inactive sulfur compounds. These pollutants highlight the need for advanced pretreatment methods and robust catalyst designs to ensure efficient and durable seawater electrolysis systems.

Further research is needed to address the remaining challenges related to fouling, corrosion, and stability in real-world conditions. Advanced membranes that prevent contamination while maintaining catalytic activity will be essential for enabling continuous operation over extended periods. Collaboration between academic institutions and industry will play a critical role in refining catalyst materials, scaling up HSEs, and ensuring the successful transition from laboratory research to industrial applications. With sustained innovation and development, seawater electrolysis has the potential to revolutionize hydrogen production, driving the global transition toward a sustainable and renewable energy economy.

DECLARATIONS

Authors' contributions

Supervised the project: Oh, M. H.; Jang, H. W.

Wrote the manuscript and contributed equally: Kim, J.; Seo, J. H.; Lee, J. K.

All authors discussed the results and commented on the manuscript at all stages.

Availability of data and materials

Not applicable.

Financial support and sponsorship

This work was financially supported by the KRISS (Korea Research Institute of Standards and Science) MPI Lab. Program. It also received funding from the Nano & Material Technology Development Program through the National Research Foundation of Korea (NRF) supported by the Ministry of Science and ICT (RS-2024-00405016). Research facilities were provided by the Inter-University Semiconductor Research Center and Institute of Engineering Research at Seoul National University. Research facilities were provided by the Inter-University Semiconductor Research Center, Institute of Engineering Research, and SOFT foundry institute at Seoul National University.

Conflicts of interest

Jang, H. W. is an Editorial Board Member of the journal *Energy Materials* but is not involved in any steps of editorial processing, notably including reviewer selection, manuscript handling, or decision-making, while the other authors have declared that they have no conflicts of interest.

Ethical approval and consent to participate

Not applicable.

Consent for publication

Not applicable.

Copyright

© The Author(s) 2025.

REFERENCES

- Bradshaw, A.; Schleicher, K. Electrical conductivity of seawater. *IEEE. J. Ocean. Eng.* **1980**, 5, 50-62. DOI
- Yu, Z.; Liu, L. Recent advances in hybrid seawater electrolysis for hydrogen production. *Adv. Mater.* **2024**, 36, e2308647. DOI
- Liu, G.; Xu, Y.; Yang, T.; Jiang, L. Recent advances in electrocatalysts for seawater splitting. *Nano. Mater. Sci.* **2023**, 5, 101-16. DOI
- Fei, H.; Liu, R.; Liu, T.; et al. Direct seawater electrolysis: from catalyst design to device applications. *Adv. Mater.* **2024**, 36, e2309211. DOI
- Hu, H.; Wang, X.; Attfield, J. P.; Yang, M. Metal nitrides for seawater electrolysis. *Chem. Soc. Rev.* **2024**, 53, 163-203. DOI
- Tong, W.; Forster, M.; Dionigi, F.; et al. Electrolysis of low-grade and saline surface water. *Nat. Energy.* **2020**, 5, 367-77. DOI
- Xiao, X.; Yang, L.; Sun, W.; et al. Electrocatalytic water splitting: from harsh and mild conditions to natural seawater. *Small* **2022**, 18, e2105830. DOI
- Liu, Y.; Wang, Y.; Fornasiero, P.; Tian, G.; Strasser, P.; Yang, X. Long-term durability of seawater electrolysis for hydrogen: from catalysts to systems. *Angew. Chem. Int. Ed.* **2024**, 136, e202412087. DOI
- Karlsson, R. K.; Cornell, A. Selectivity between oxygen and chlorine evolution in the chlor-alkali and chlorate processes. *Chem. Rev.* **2016**, 116, 2982-3028. DOI PubMed
- Bahuguna, G.; Patolsky, F. Routes to avoiding chlorine evolution in seawater electrolysis: recent perspective and future directions. *ACS. Mater. Lett.* **2024**, 6, 3202-17. DOI
- Bahuguna, G.; Patolsky, F. Why today's "water" in water splitting is not natural water? Critical up-to-date perspective and future challenges for direct seawater splitting. *Nano. Energy.* **2023**, 117, 108884. DOI
- Haq, T. U.; Haik, Y. Strategies of anode design for seawater electrolysis: recent development and future perspective. *Small. Sci.* **2022**, 2, 2200030. DOI
- Liang, J.; Li, Z.; He, X.; et al. Electrocatalytic seawater splitting: nice designs, advanced strategies, challenges and perspectives. *Mater. Today.* **2023**, 69, 193-235. DOI
- Gouda, V. K.; Banat, I. M.; Riad, W. T.; Mansour, S. Microbiologically induced corrosion of UNS N04400 in seawater. *Corrosion* **1993**, 49, 63-73. DOI
- Oh, B. S.; Oh, S.; Jung, Y. J.; Hwang, Y.; Kang, J.; Kim, I. S. Evaluation of a seawater electrolysis process considering formation of free chlorine and perchlorate. *Desalination. Water. Treat.* **2010**, 18, 245-50. DOI
- Kang, X.; Yang, F.; Zhang, Z.; et al. A corrosion-resistant RuMoNi catalyst for efficient and long-lasting seawater oxidation and anion exchange membrane electrolyzer. *Nat. Commun.* **2023**, 14, 3607. DOI PubMed PMC
- Park, Y. S.; Jeong, J.; Jang, M. J.; et al. Ternary layered double hydroxide oxygen evolution reaction electrocatalyst for anion exchange membrane alkaline seawater electrolysis. *J. Energy. Chem.* **2022**, 75, 127-34. DOI
- Yang, P.; Liu, F.; Zang, X.; et al. Microwave quasi-solid state to construct strong metal-support interactions with interfacial electron-enriched Ru for anion exchange membrane electrolysis. *Adv. Energy. Mater.* **2024**, 14, 2303384. DOI
- Hu, H.; Zhang, Z.; Liu, L.; et al. Efficient and durable seawater electrolysis with a V₂O₃-protected catalyst. *Sci. Adv.* **2024**, 10, eadn7012. DOI PubMed PMC
- Chang, J.; Wang, G.; Yang, Z.; et al. Dual-doping and synergism toward high-performance seawater electrolysis. *Adv. Mater.* **2021**, 33, e2101425. DOI
- Xia, Y.; Guo, L.; Zhu, J.; et al. Manipulating electronic structure of nickel phosphide via asymmetric coordination interaction for anion-exchange membrane based seawater electrolysis. *Appl. Catal. B. Environ. Energy.* **2024**, 351, 123995. DOI
- Song, L.; Guo, L.; Mao, J.; et al. Boosting hydrogen adsorption via manipulating the d-band center of ferroferric oxide for anion exchange membrane-based seawater electrolysis. *ACS. Catal.* **2024**, 14, 6981-91. DOI
- Wang, H.; Jiang, N.; Huang, B.; Yu, Q.; Guan, L. Surface amorphization and functionalization of a NiFeOOH electrocatalyst for a robust seawater electrolyzer. *EES. Catal.* **2024**, 2, 1092-9. DOI
- Li, Q.; Fu, X.; Li, H.; et al. Strong d-p orbital hybridization of Os-P via ultrafast microwave plasma assistance for anion exchange membrane electrolysis. *Adv. Funct. Mater.* **2024**, 34, 2408517. DOI
- Cui, T.; Chi, J.; Liu, K.; et al. Manipulating the electron redistribution of Fe₃O₄ for anion exchange membrane based alkaline seawater electrolysis. *Appl. Catal. B. Environ. Energy.* **2024**, 357, 124269. DOI
- Jun, S. E.; Myeong, S.; Cho, B.; et al. Exsolved Ru-mediated stabilization of MoO₂-Ni₄Mo electrocatalysts for anion exchange membrane water electrolysis and unbiased solar-driven saline water splitting. *Appl. Catal. B. Environ. Energy.* **2024**, 358, 124364. DOI
- Lee, S. A.; Bu, J.; Lee, J.; Jang, H. W. High-entropy nanomaterials for advanced electrocatalysis. *Small. Sci.* **2023**, 3, 2200109. DOI
- Choi, D.; Ryu, S. Efficient and selective oxygen evolution reaction in seawater electrolysis with electrochemically synthesized amorphous-like NiFeS. *Electron. Mater. Lett.* **2024**, 20, 173-82. DOI
- Cho, Y. B.; Nguyen, D. C.; Hua, S. H.; Kim, Y. S. Direct detection of water-dissolved ammonia using paper-based analytical devices. *J. Sensor. Sci. Technol.* **2023**, 32, 67-74. DOI
- Kim, J.; Kang, D.; Kim, S.; Jang, H. W. Catalyze materials science with machine learning. *ACS. Mater. Lett.* **2021**, 3, 1151-71. DOI
- Vos, J. G.; Wezendonk, T. A.; Jeremiasse, A. W.; Koper, M. T. M. MnO_x/IrO_x as selective oxygen evolution electrocatalyst in acidic chloride solution. *J. Am. Chem. Soc.* **2018**, 140, 10270-81. DOI PubMed PMC
- Hu, H.; Zhang, Z.; Zhang, Y.; et al. An ultra-low Pt metal nitride electrocatalyst for sustainable seawater hydrogen production. *Energy.*

- Environ. Sci.* **2023**, *16*, 4584-92. DOI
33. Veroneau, S. S.; Nocera, D. G. Continuous electrochemical water splitting from natural water sources via forward osmosis. *Proc. Natl. Acad. Sci. USA*. **2021**, *118*, e2024855118. DOI PubMed PMC
34. Desai, D.; Beh, E. S.; Sahu, S.; et al. Electrochemical desalination of seawater and hypersaline brines with coupled electricity storage. *ACS. Energy. Lett.* **2018**, *3*, 375-9. DOI
35. Loutatidou, S.; Chalermthai, B.; Marpu, P. R.; Arafat, H. A. Capital cost estimation of RO plants: GCC countries versus southern Europe. *Desalination* **2014**, *347*, 103-11. DOI
36. Logan, B. E.; Shi, L.; Rossi, R. Enabling the use of seawater for hydrogen gas production in water electrolyzers. *Joule* **2021**, *5*, 760-2. DOI
37. Lee, J. K.; Seo, J. H.; Lim, J.; Park, S.; Jang, H. W. Best practices in membrane electrode assembly for water electrolysis. *ACS. Mater. Lett.* **2024**, *6*, 2757-86. DOI
38. Abbasi, R.; Setzler, B. P.; Lin, S.; et al. A roadmap to low-cost hydrogen with hydroxide exchange membrane electrolyzers. *Adv. Mater.* **2019**, *31*, e1805876. DOI
39. Li, J.; Sun, J.; Li, Z.; Meng, X. Recent advances in electrocatalysts for seawater splitting in hydrogen evolution reaction. *Int. J. Hydrogen. Energy*. **2022**, *47*, 29685-97. DOI
40. Lee, S. A.; Kim, J.; Kwon, K. C.; Park, S. H.; Jang, H. W. Anion exchange membrane water electrolysis for sustainable large-scale hydrogen production. *Carbon. Neutral.* **2022**, *1*, 26-48. DOI
41. Vincent, I.; Bessarabov, D. Low cost hydrogen production by anion exchange membrane electrolysis: a review. *Renew. Sustain. Energy. Rev.* **2018**, *81*, 1690-704. DOI
42. Shao, L.; Han, X.; Shi, L.; et al. In situ generation of molybdate-modulated nickel-iron oxide electrodes with high corrosion resistance for efficient seawater electrolysis. *Adv. Energy. Mater.* **2024**, *14*, 2303261. DOI
43. Xu, W.; Wang, Z.; Liu, P.; et al. Ag nanoparticle-induced surface chloride immobilization strategy enables stable seawater electrolysis. *Adv. Mater.* **2024**, *36*, e2306062. DOI
44. Zhang, S.; Xu, W.; Chen, H.; et al. Progress in anode stability improvement for seawater electrolysis to produce hydrogen. *Adv. Mater.* **2024**, *36*, e2311322. DOI
45. Huang, C.; Zhou, Q.; Yu, L.; et al. Functional bimetal Co-modification for boosting large-current-density seawater electrolysis by inhibiting adsorption of chloride ions. *Adv. Energy. Mater.* **2023**, *13*, 2301475. DOI
46. Gong, Z.; Liu, J.; Yan, M.; Gong, H.; Ye, G.; Fei, H. Highly durable and efficient seawater electrolysis enabled by defective graphene-confined nanoreactor. *ACS. Nano*. **2023**, *17*, 18372-81. DOI
47. Fan, R.; Liu, C.; Li, Z.; et al. Ultrastable electrocatalytic seawater splitting at ampere-level current density. *Nat. Sustain.* **2024**, *7*, 158-67. DOI
48. Liu, J.; Liu, X.; Shi, H.; et al. Breaking the scaling relations of oxygen evolution reaction on amorphous NiFeP nanostructures with enhanced activity for overall seawater splitting. *Appl. Catal. B. Environ.* **2022**, *302*, 120862. DOI
49. Liu, H.; Shen, W.; Jin, H.; et al. High-performance alkaline seawater electrolysis with anomalous chloride promoted oxygen evolution reaction. *Angew. Chem. Int. Ed.* **2023**, *62*, e202311674. DOI
50. Zhao, Y.; Adiyari, S. D. P.; Huang, C.; et al. Oxygen evolution/reduction reaction catalysts: from in situ monitoring and reaction mechanisms to rational design. *Chem. Rev.* **2023**, *123*, 6257-358. DOI
51. Dionigi, F.; Reier, T.; Pawolek, Z.; Gliech, M.; Strasser, P. Design criteria, operating conditions, and nickel-iron hydroxide catalyst materials for selective seawater electrolysis. *ChemSusChem* **2016**, *9*, 962-72. DOI PubMed
52. Guo, J.; Zheng, Y.; Hu, Z.; et al. Direct seawater electrolysis by adjusting the local reaction environment of a catalyst. *Nat. Energy*. **2023**, *8*, 264-72. DOI
53. Dresp, S.; Dionigi, F.; Loos, S.; et al. Direct electrolytic splitting of seawater: activity, selectivity, degradation, and recovery studied from the molecular catalyst structure to the electrolyzer cell level. *Adv. Energy. Mater.* **2018**, *8*, 1800338. DOI
54. Jung, H.; Song, J.; Lee, Y.; et al. Computational discovery of optimal dopants for nickel iron oxyhydroxide to enhance OER activity and saline water compatibility. *ACS. Energy. Lett.* **2024**, *9*, 2162-72. DOI
55. Zhang, S.; Wang, Y.; Li, S.; et al. Concerning the stability of seawater electrolysis: a corrosion mechanism study of halide on Ni-based anode. *Nat. Commun.* **2023**, *14*, 4822. DOI PubMed PMC
56. Dresp, S.; Dionigi, F.; Klingenhof, M.; Strasser, P. Direct electrolytic splitting of seawater: opportunities and challenges. *ACS. Energy. Lett.* **2019**, *4*, 933-42. DOI
57. Han, J.; Jwa, E.; Lee, H.; et al. Direct seawater electrolysis via synergistic acidification by inorganic precipitation and proton flux from bipolar membrane. *Chem. Eng. J.* **2022**, *429*, 132383. DOI
58. Li, T.; Zhao, X.; Getaye, S. M.; et al. Phosphate-decorated Ni₃Fe-LDHs@CoPx nanoarray for near-neutral seawater splitting. *Chem. Eng. J.* **2023**, *460*, 141413. DOI
59. Li, J.; Yu, T.; Wang, K.; et al. Multiscale engineering of nonprecious metal electrocatalyst for realizing ultrastable seawater splitting in weakly alkaline solution. *Adv. Sci.* **2022**, *9*, e2202387. DOI PubMed PMC
60. Cai, Z.; Liang, J.; Li, Z.; et al. Stabilizing NiFe sites by high-dispersity of nanosized and anionic Cr species toward durable seawater oxidation. *Nat. Commun.* **2024**, *15*, 6624. DOI PubMed PMC
61. Li, P.; Zhao, S.; Huang, Y.; Huang, Q.; Yang, Y.; Yang, H. Multiscale structural engineering of a multilayered nanoarray electrode realizing boosted and sustained oxygen evolution catalysis in seawater electrolysis. *ACS. Catal.* **2023**, *13*, 15360-74. DOI

62. Khan, M. A.; Al-Attas, T.; Roy, S.; et al. Seawater electrolysis for hydrogen production: a solution looking for a problem? *Energy. Environ. Sci.* **2021**, 14, 4831-9. DOI
63. Karoui, H.; Riffault, B.; Jeannin, M.; et al. Electrochemical scaling of stainless steel in artificial seawater: role of experimental conditions on CaCO_3 and $\text{Mg}(\text{OH})_2$ formation. *Desalination* **2013**, 311, 234-40. DOI
64. Kang, W.; Meng, S.; Zhao, Y.; et al. Scaling-free cathodes: enabling electrochemical extraction of high-purity nano- CaCO_3 and - $\text{Mg}(\text{OH})_2$ in seawater. *Environ. Sci. Technol.* **2024**, 58, 14034-41. DOI
65. Yi, L.; Chen, X.; Wen, Y.; et al. Solidophobic surface for electrochemical extraction of high-valued $\text{Mg}(\text{OH})_2$ coupled with H_2 production from seawater. *Nano. Lett.* **2024**, 24, 5920-8. DOI
66. Lee, S.; Kim, E.; Lee, D.; Jang, K.; Park, J.; Choi, W. Y. Synthesis of seawater-derived superhydrophobic calcium carbonate via CO_2 mineralization by utilizing L-Arginine/L-Lysine oleate-based self-assembly structures. *Chem. Eng. J.* **2024**, 490, 151785. DOI
67. Drespe, S.; Ngo, T. T.; Klingenhof, M.; Brückner, S.; Hauke, P.; Strasser, P. Efficient direct seawater electrolyzers using selective alkaline NiFe-LDH as OER catalyst in asymmetric electrolyte feeds. *Energy. Environ. Sci.* **2020**, 13, 1725-9. DOI
68. Zhou, Z.; Pei, Z.; Wei, L.; Zhao, S.; Jian, X.; Chen, Y. Electrocatalytic hydrogen evolution under neutral pH conditions: current understandings, recent advances, and future prospects. *Energy. Environ. Sci.* **2020**, 13, 3185-206. DOI
69. Rodriguez-blanco, J.; Shaw, S.; Bots, P.; Roncal-herrero, T.; Benning, L. The role of pH and Mg on the stability and crystallization of amorphous calcium carbonate. *J. Alloys. Compd.* **2012**, 536, S477-9. DOI
70. Yousefi, S.; Ghasemi, B.; Tajally, M.; Asghari, A. Optical properties of MgO and $\text{Mg}(\text{OH})_2$ nanostructures synthesized by a chemical precipitation method using impure brine. *J. Alloys. Compd.* **2017**, 711, 521-9. DOI
71. Chen, H.; Liu, P.; Li, W.; et al. Stable seawater electrolysis over 10 000 h via chemical fixation of sulfate on NiFeBa-LDH. *Adv. Mater.* **2024**, 36, e2411302. DOI
72. Liao, L.; Li, D.; Zhang, Y.; et al. Complementary multisite turnover catalysis toward superefficient bifunctional seawater splitting at ampere-level current density. *Adv. Mater.* **2024**, 36, e2405852. DOI
73. Liu, X.; Chi, J.; Mao, H.; Wang, L. Principles of designing electrocatalyst to boost reactivity for seawater splitting. *Adv. Energy. Mater.* **2023**, 13, 2301438. DOI
74. Tlili, M. M.; Benamor, M.; Gabrielli, C.; Perrot, H.; Tribollet, B. Influence of the interfacial pH on electrochemical CaCO_3 precipitation. *J. Electrochem. Soc.* **2003**, 150, C765. DOI
75. Zheng, W.; Lee, L. Y. S.; Wong, K. Y. Improving the performance stability of direct seawater electrolysis: from catalyst design to electrode engineering. *Nanoscale* **2021**, 13, 15177-87. DOI
76. Liu, J.; Duan, S.; Shi, H.; et al. Rationally designing efficient electrocatalysts for direct seawater splitting: challenges, achievements, and promises. *Angew. Chem. Int. Ed.* **2022**, 61, e202210753. DOI
77. Xie, H.; Zhao, Z.; Liu, T.; et al. A membrane-based seawater electrolyzer for hydrogen generation. *Nature* **2022**, 612, 673-8. DOI
78. Adisasmito, S.; Khoiruddin, K.; Sutrisna, P. D.; Wenten, I. G.; Siagian, U. W. R. Bipolar membrane seawater splitting for hydrogen production: a review. *ACS. Omega.* **2024**, 9, 14704-27. DOI PubMed PMC
79. Zheng, Y.; Qiao, S. Direct seawater splitting to hydrogen by a membrane electrolyzer. *Joule* **2023**, 7, 20-2. DOI
80. Jin, H.; Xu, J.; Liu, H.; et al. Emerging materials and technologies for electrocatalytic seawater splitting. *Sci. Adv.* **2023**, 9, eadi7755. DOI PubMed PMC
81. Liang, J.; Cai, Z.; He, X.; et al. Electroreduction of alkaline/natural seawater: self-cleaning Pt/carbon cathode and on-site co-synthesis of H_2 and Mg hydroxide nanoflakes. *Chem* **2024**, 10, 3067-87. DOI
82. Zhao, L.; Zhou, S.; Lv, Z.; et al. Anti-precipitation molecular metal chalcogenide complexes modification for efficient direct alkaline seawater splitting at the large current density. *Appl. Catal. B. Environ.* **2023**, 338, 122996. DOI
83. Yang, C.; Wu, Z.; Zheng, Y.; et al. Electron-donating Cu atoms induced high proton supply and anti-poisoning ruthenium clusters for superior direct seawater hydrogen production. *Adv. Funct. Mater.* **2024**, 34, 2404061. DOI
84. Liang, J.; Cai, Z.; Li, Z.; et al. Efficient bubble/precipitate traffic enables stable seawater reduction electrocatalysis at industrial-level current densities. *Nat. Commun.* **2024**, 15, 2950. DOI PubMed PMC
85. Jwa, E.; Kim, H.; Chon, K.; et al. Bioelectrochemical precipitation system for removal of scale-forming ions from seawater using two different buffers. *Desalination* **2017**, 418, 35-42. DOI
86. Ren, Y.; Fan, F.; Zhang, Y.; et al. A Dual-cation exchange membrane electrolyzer for continuous H_2 production from seawater. *Adv. Sci.* **2024**, 11, e2401702. DOI PubMed PMC
87. Shi, H.; Wang, T.; Liu, J.; et al. A sodium-ion-conducted asymmetric electrolyzer to lower the operation voltage for direct seawater electrolysis. *Nat. Commun.* **2023**, 14, 3934. DOI PubMed PMC
88. Li, T.; Wang, B.; Cao, Y.; et al. Energy-saving hydrogen production by seawater electrolysis coupling tip-enhanced electric field promoted electrocatalytic sulfon oxidation. *Nat. Commun.* **2024**, 15, 6173. DOI PubMed PMC
89. Sun, F.; Qin, J.; Wang, Z.; et al. Energy-saving hydrogen production by chlorine-free hybrid seawater splitting coupling hydrazine degradation. *Nat. Commun.* **2021**, 12, 4182. DOI PubMed PMC